IEEE/CSC & ESAS EUROPEAN SUPERCONDUCTIVITY NEWS FORUM (global edition), October 2016.
Invited presentation 1LOr2A-02 given at ASC 2016; Denver,Colorado,USA, September 4 – 9, 2016.

1st Performance Test of the 25 T Cryogen-free Superconducting Magnet

Satoshi Awaji, Kazuo Watanabe, Hidetoshi Oguro, Hiroshi Miyazaki, Satoshi Hanai, Taizo Tosaka, Shigeru Ioka

***Abstract*—A 25 T cryogen-free superconducting magnet (25T-CSM) was developed and installed at the High Field Laboratory for Superconducting Materials (HFLSM), IMR, Tohoku University. It consists of an inner high temperature superconducting (HTS), a middle CuNb/Nb_3Sn Rutherford cable and an outer NbTi Rutherford cable coils. All the coils are impregnated by an epoxy resin for conduction cooling. Though initially the $GdBa_2Cu_3O_y$ (Gd123) coil was designed as the HTS insert coil, the $Bi_2Sr_2Ca_2Cu_3O_y$ (Bi2223) coil was also developed. The HTS insert and the LTS (CuNb/Nb_3Sn and NbTi) outsert coils are cooled by two 4K GM and two GM/JT cryocoolers, respectively. The LTS coils successfully generated a 14 T by an operation current of 854 A without any training quench. The Gd123 coil generated 10.15 T by 132.6 A in an absence of background field. And then the operation current of the Gd123 insert was increased step-by-step in a background field. The Gd123 coil could be operated up to 124.0 A stably, which corresponds to a 23.55 T, but quenched around 124.6 A (23.61 T), under the background field of 14 T. The Bi2223 insert coil using the Ni-alloy reinforced Bi2223 tapes successfully generated 11.48 T by 204.7A in a stand-alone operation and 24.57 T in a background field of 14 T. The differences between the calculated and the measured values of the central magnetic fields are about 0.4 T for the Gd123 insert and 0.1 T for the Bi2223 one around 24 T.**

***Index Terms*—high field magnet, cryogen-free superconducting magnet, quench, REBCO tape, BSCCO tape, large hoop stress**

I. Introduction

HIGH field superconducting magnets beyond 20 T are under development using high temperature superconductors (HTSs) recently [1, 2, 3]. This is because of the HTS practical tapes with high strength and high in-field critical current density J_c. In particular, $REBa_2Cu_3O_y$ (RE123, RE: rare-earth and Y) coated conductors with a Hastelloy substrates are one of most promising HTS tapes because of the high mechanical strength [4]. In fact, a 32 T all superconducting magnet is under construction using a RE123 insert coil [2]. Recently 27 T was recorded by the prototype RE123 insert coils for the 32 T superconducting magnet combined with a 14 T LTS outsert. [5]. In addition, all RE123 magnet made by a non-insulation technology was developed and it generated a 26.4 T [6]. These bear out a high performance of RE123 coil for high magnetic field generation.

On the other hand, it is well known that a silver sheathed $Bi_2Sr_2Ca_2Cu_3O_y$ (Ag/Bi2223) tape has also large in-field J_c at low temperatures below 20 K but the low mechanical property was remained as a problem for the high field magnets. Recently, the high strength Ag/Bi2223 tapes reinforced by a Cu-alloy (CA), a stainless steel (SS) and a Ni-alloy (Nx) with a pre-tension were developed by Sumitomo Electric Industry [6, 7]. By using the CA/Ag/Bi2223 tapes, we succeed in an upgrading to 20T cryogen-free superconducting magnet (20T-CSM) from the 18T-CSM with 52 room temperature bore [8, 9]. Now it is routinely used for many users at the HFLSM, IMR, Tohoku University [10]. The 24T (1020 MHz) NMR magnet was also developed using a CA/Ag/Bi2223 insert coil last year at the National Institute for Materials Science (NIMS) [11]. They succeeded in the observation of 1020 MHz NMR signals.

We were developing the 25T-CSM since 2013 under the "High Magnetic Field Collaboratory in Japan" project established in 2012 at the Science council of Japan. The 25T-CSM development project was done as an R&D for a future 30 T superconducting magnet and 50 T-class hybrid magnet.

Recently we installed and carried out performance tests of the 25T-CSM. The 1st performance test results of the 25T-CSM are reported in this paper.

II. Coil Design

The 25 T-CSM consists of HTS insert, Nb_3Sn middle and NbTi outer coils. In order to realize compact coils for the conduction cooling, we adopted high strength design [1]. Total stored energy is about 12 MJ at 25.5 T. In addition, the HTS and the LTS (Nb_3Sn and NbTi) coils are thermally separated and cooled by two 4K GM- and two GM/JT cryocoolers, respectively. The detailed designs are shown in following subsections separately.

A. LTS coils [14]

The specifications of the LTS coil consists of three NbTi (L4a, L4b and L5) and three Nb_3Sn (L1-L3) coils as shown in Table 1. All LTS coils were solenoid coils impregnated by epoxy. The NbTi coils are wound using the Rutherford cables. The NbTi Rutherford cables are made by 16 strands with 0.7 mm and 0.8 mm diameters. The critical current I_c of the NbTi strands are 316-317 A and 240-250 A at 4.2 K and 7 T for the

A part of this work was supported by the Japan Society for the Promotion of Science through the Grant-in-Aid for Scientific Research (A) under KAKENHI 25246032.

S. Awaji, H. Oguro and K. Watanabe are with High Field Laboratory for Superconducting Materials, Institute for Material Research, Tohoku University. Sendai 980-8577, Japan. (phone: +81-22-215-2151; fax: +81-22-215-2149; e-mail: awaji@imr.tohoku.ac.jp). The present address of H. Oguro is Tokai University, Japan.
H. Miyazaki, S. Hanai, T. Tosaka and S. Ioka are with Toshiba Corporation, Yokohama 230-0045, Japan.

TABLE I
DESIGN OF LOW TEMPERATURE SUPERCONDUCTING (LTS) COIL OF 25 T-CSM

Coil	L1	L2	L3	L4a	L4b	L5
Cable type	CuNb/Nb_3Sn Rutherford			Cu/NbTi Rutherford		
No of strands	ϕ0.8 x 16			ϕ0.8 x 16	ϕ0.7 x 16	
Operating current (A)	854					
Inner radius (mm)	149.5	185.3	228.6	271.7	301.6	312.9
Outer radius (mm)	182.9	226.4	270.1	301.6	311.9	356.3
Coil height (mm)	542.0	630.3	630.4	629.5	629.5	629.5
Coil current density (A/mm^2)	67.6	67.4	66.7	68.9	84.7	86.7
No of turns	1438	2043	2043	1518	641	2779
B_{max} (T)	13.8	11.3	8.4	6.8	6.2	5.9
B_0 (T)	2.43	2.91	2.73	1.91	0.78	3.25
Conductor width (mm)	6.45			6.30	5.57	5.57
Conductor thickness (mm)	1.53			1.50	1.31	1.31
Conductor current density (A/mm^2)	106.2			106.2	138.6	138.6
T_{cs} (K)	6.69	8.37	9.94	5.98	6.20	6.39
Axial compressive stress (MPa)	38	50	48	47	55	92
Maximum hoop stress (MPa)	252	244	202	138	113	52

TABLE II
SPECIFICATION OF THE HIGH TEMPERATURE SUPERCONDUCTING (HTS) COILS OF 25 T-CSM

Coil	H1-Gd	H1-Bi
Material	$GdBa_2Cu_3O_y$	$Bi_2Sr_2Ca_2Cu_3O_y$
Conductor size (mm)	^{w}5.00 x ^{t}0.13	^{w}4.50 x ^{t}0.31
I_c (77.3K, sf)	> 250 A	> 185 A
Total tape length (m)	13960	11454
Insulation thickness (mm)	0.055	0.07
Operating current (A)	144	203
Inner radius (mm)	52	47.9
Outer radius (mm)	131.4	138.9
Coil height (mm)	336	389.1
Coil current density (A/mm^2)	221.5	111.9
No of pancakes	56SP	38DP
No of turns/SP	435	257
B_{max} (T)	25.6	25.6
B_r (T)	4.66	4.14
B_0 (T)	11.5	11.50
Conductor current density (A/mm^2)	129.8	150.4
Axial compressive stress (MPa)	32	32
Maximum hoop stress (MPa)	407	323

SP: Single pancake, DP: Double pancake

0.7 mm and the 0.8 mm diameter strands, respectively.

High strength Nb_3Sn strands reinforced by a Nb-rod processed Cu-20wt%Nb (CuNb/Nb_3Sn) were adopted for the Nb_3Sn Rutherford cables [12]. The Rutherford cable composed of 16 CuNb/Nb_3Sn strands were used for the Nb_3Sn coils. All the Nb_3Sn solenoid coils were made by react-and-wind (R&W) method. In addition, we applied pre-bending treatment to the reacted Rutherford Nb_3Sn cables before the winding. In this case, the double bending strain of 0.5% at room temperature were applied 5 times using pulleys to improve I_c [13, 14]. As a result, the load factor of the L1 coil, which is operated in the most severe condition, is 0.49%. The maximum hoop and transverse compressive stresses are about 250 MPa and 50 MPa, respectively. This high stress design is a challenging attempt in the Nb_3Sn magnet. We confirmed that the internal strain of Nb_3Sn in the Rutherford cables for both axial and transverse directions under the external stress are different with the macroscopic strain because of the twisted structures [15]. It is expected that it becomes a margin of the high stress operation [16].

B. HTS insert coil

We made two HTS insert coils using the Cu/Ag/Gd123/Hastelloy and Ni-Alloy/Ag/Bi2223 (Type HT-Nx) tapes, respectively. Both are designed on 11.5 T in a background field of 14 T by the LTS coils, so as to generate the maximum field of 25.5 T. The final designs of HTS inserts for the 25 T-CSM are shown in Table II.

Gd123 insert coil [17]

Cu-plated Gd123 tapes with a 70 μm thick Hastelloy substrate were provided from Fujikura Ltd. for the Gd123 insert. The I_c of Gd123 tapes are 236 A to 355 A at 77.3 K and self-field. Total length of Gd123 tapes used for the Gd123 insert is approximately 14 km. All single pancakes were impregnated by an epoxy resin for good thermal conduction. In order to avoid the degradation due to the delamination stress, all turns are separated mechanically by cowinding a Teflon coated polyimide insulation tape [18, 19]. We measured the coils I_c values of all single pancakes and double stacked pancakes in immersing liquid N_2 and then stacked those so that small I_c coils locate near the center of the insert. The maximum hoop stress is about 407 MPa at 25.5 T and 366 MPa at 24.5 T. The stress limit of the Gd123 tape determined by the 95% I_c degradation is about 800 MPa at 77.3 K [1]. This is higher than that of the Cu-laminated Gd123 tapes in Fujikura [4]. The detailed design, fabrication and stand-alone test results are described in ref. 17.

Bi2223 insert coil [20]

High strength Ni-alloy laminated silver sheathed Bi2223 tapes (Type HT-Nx) newly developed by Sumitomo Electric Industry Ltd. were adopted for the Bi2223 insert of the 25T-CSM [6]. The Bi2223 double pancake coils were partially impregnated to reduce the maximum hoop stress and make a good thermal conductivity at the same time. The turn-separation was given from 51 to 186 turns using the Teflon

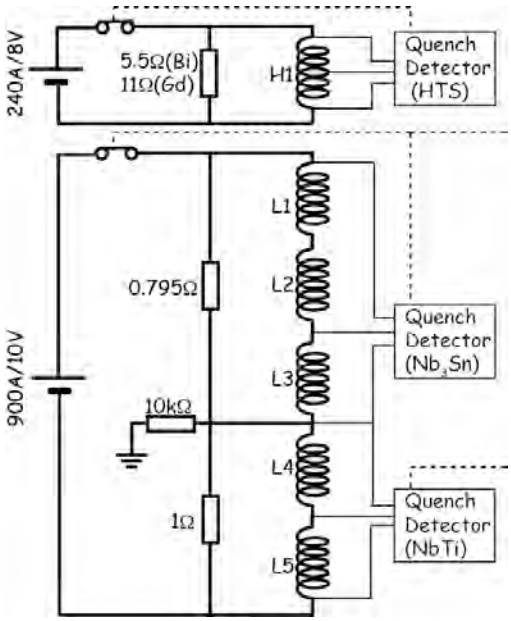

Fig. 1. Schematic electric cuircuit including the quench detectiona and protection circuits.

coated polyimide tape insulation as well as the Gd123 coils. The partial turn-separation reduces the maximum hoop stress from 463 MPa to 323 MPa. Since the strength of the type HT-Nx Bi2223 tape is about 400 MPa at 77.3 K, the designed maximum hoop stress is below the limit with about a 20% margin. We made 39 double pancake coils and measured the coil I_c of them in immersing liquid N_2. The coil I_c of the all coils were almost the same as 70 A at 77.3 K and self-field. Two of the Bi2223 double pancakes were used for a R&D coil for a hoop stress test [21]. The detailed design, fabrication and performance test results are described in ref. 21.

III. Quench Detection and Protection

The schematic electrical circuit including the protection and detection circuits is shown in Fig. 1. The balance voltages are utilized for quench detection systems of the HTS and the Nb_3Sn and NbTi coils separately. When the balance voltages would be over adequate criteria, the circuit barkers of all coils are opened and the operation current starts to dump. The dump resistances are 11 Ω for the Gd123 coil, 5.5 Ω for the Bi2223 coil, 0.795 Ω for the Nb_3Sn and 1 Ω for the NbTi coils. The dump resistance values were determined so that the maximum induced currents are below the critical currents at 20 K in the HTS coils and the induced voltages become smaller than 1500 V. We set the quench heater to accelerate the quench propagation only in the LTS coils.

IV. Cooling Design [21]

The HTS coil and the LTS coil are operated by individual power supplies and are cooled separately by different cooing systems, in order to allow the temperature rise of the HTS coil during energizing. It saves the cost of cooling system due to the larger cooling power at higher temperature of the GM cryocooler. We use two 4K-GM cryocoolers for the HTS coils, two GM/JT cryocoolers for the LTS coils and two single-stage GM cryocoolers for radiation shield and the high temperature ends of HTS current leads. In addition, In order to reduce an effect of strayed field, the cryocoolers are set at the one side of the oval-shaped cryostat to make a distance from the coils, which locate at the another side in the cryostat. We use the He circulations to carry the heat from the coils and cryocoolers. The heat exchangers located at the top and bottom of coils are cooled by the helium gas or liquid. The all pancake coils are connected to either heat-exchangers by high purity aluminum sheets.

We equipped difference sequences of cooling path for the initial cooling from room temperature. By changing the cooling paths, we can cool both HTS and LTS coils with a similar cooling rate using all cryocoolers efficiently [21]. The AC-losses in the HTS coils are also important issues. The estimated averaged AC-losses are from a few watts to 10 W at a one-hour energization to 25 T, although those depend on the model [17, 22]. However, those can be covered by larger cooling power of 4K-GM cryocooler at higher temperature. In fact, the cooling power of the 4K GM cryocooler becomes about 10 W at 8 K from 1.5 W at 4.2 K [23]. Detailed cooling design and test results are presented in ref. 21.

Fig. 2. Photo of the 25T-CSM installed at the HFLSM anex buliding.

V. Test Results

The 25T-CSM was installed at the High Field Laboratory for Superconducting Materials (HFSLM), Institute for Materials Research (IMR), Tohoku University as shown in Fig. 2. The all installations such as compressors, gas circulation systems, power supplies, control system, quench detection systems and so on locate in the machinery room at the next of the magnet room. The balcony was made on the machinery room for experiments of users.

The magnet could be cooled at 4.3 K for the LTS coil and 4.6 K for the HTS coil from room temperature within 7 days [21]. The temperatures of the radiation shield and high temperature ends are about 40 K and 30-35 K, respectively. The cooling results indicate that the high efficient cooling system with cryocoolers works quite well.

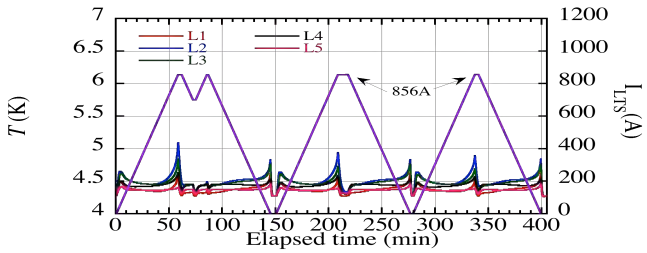

Fig. 3. Temperature profiles at the repeated charging of the LTS coils.

A. *LTS coil* [14]

The stand-alone test of LTS coil was successfully performed. Although we were afraid of the many training quenches of the LTS coil because of Rutherford cable, the 14 T was achieved without any training quench. Instead, anomalous rapid temperature rise during ramping current in high magnetic field was observed at the virgin run. It is considered that the small wire slips and movements occurred as disturbances, which has smaller energy than the minimum quench energy. From the second run, we energized a 14 T repeatedly without any anomalous temperature rises as shown in Fig. 3. The maximum temperature of the LTS coils was about 5 K for a one-hour ramping to the maximum.

B. *Gd123 insert coil* [17]

10.61 T, which was calculated, was achieved by an operation current of 132.6 A without a background field using the Gd123 insert coil [17]. In this case, the measured magnetic field by a Hall probe is 10.15 T. Hence, the 0.46 T difference between the calculated and measured fields appeared due to the shielding current effect [24].

Figure 4 shows the test results under a background field of 14 T by the LTS coil. First we generated 14 T as a background field and then energized the Gd123 coil step-by-step. The

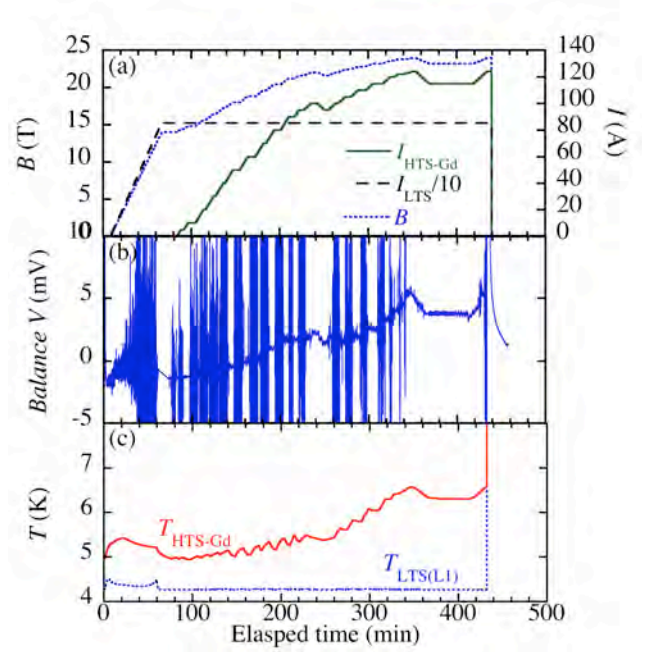

Fig. 4. Combination test results of the 25T-CSM, (a) operation current and magnetic field, (b) balance voltage and (c) temperatures.

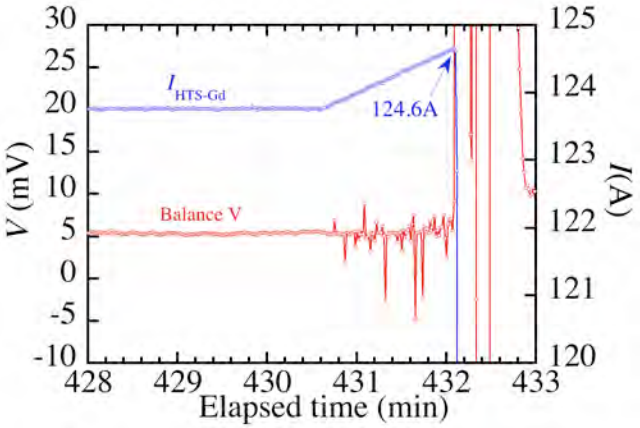

Fig. 5. Detailed balance voltage and current of the HTS-Gd coil at the quench of the 25T-CSM.

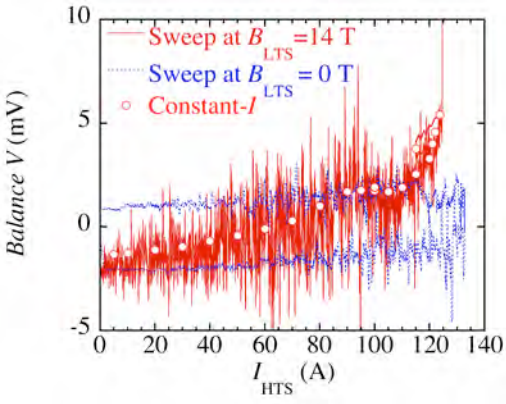

Fig. 6. *I-V* properties of the HTS-Gd insert coil in 0 T and 14 T.

balance voltage shows large and many spikes during sweeping operation current. When we stop ramping, the noise becomes small. We think those may come from the cracking and/or wire movements because of the separation of all windings. The temperature also increases with ramping but decreases when we hold the current immediately. Those may be due to the AC-losses. The coil temperature and balance voltage increased gradually with increasing current. When the current became 124 A, the coil temperature and the balance voltage reached to about 6.6 K and 5.5 mV, respectively. We decreased the current from 124 A to 115 A once and holt it. We confirmed the stable operation for about 50 min at 114 A, which corresponded to 23.2 T. Then the operation current increased again. The balance voltage rapidly increased at 124.6 A and the quench event happened due to the operation of quench detector of the HTS coil as shown in Fig. 5. The calculated magnetic field from 124.6 A is 24.01 T. Therefore, 24.01 T was achieved using the Gd123 insert just before the quench.

From the comparison of the current vs voltage properties between the combination and the stand-alone tests in Fig. 6, the small nonlinear voltages appear from a low current in 14 T. It is suggested that the thermal runaway due to the degradation of superconducting properties took place locally.

The various signals just after the quench are also shown in Fig. 7. The elapsed time in the figure is set to zero at the

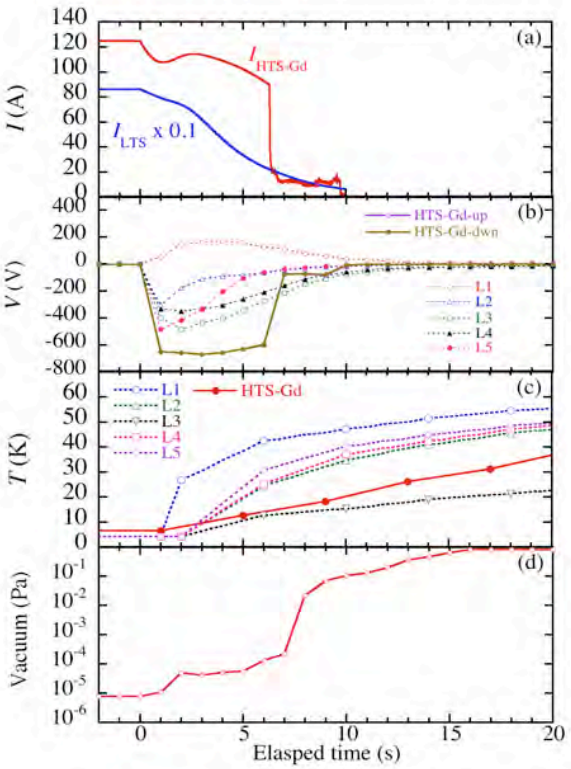

Fig. 7. HTS-Gd coil properties juast after the quench (a) Operation current, (b) Voltages, (c) Temperatures and (d) Vacuum pressure in the cryostat.

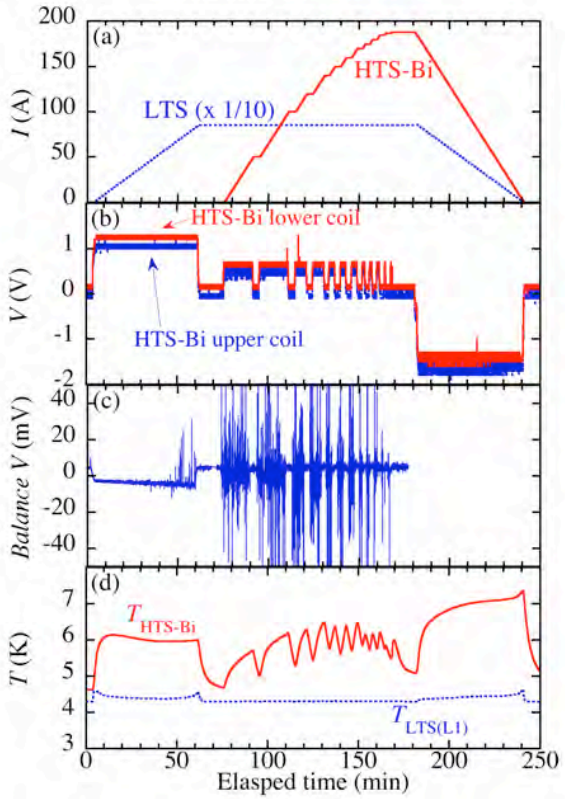

Fig. 8. HTS-Bi coil properties at the separated sweeping test (a) Operation current, (b) Voltages, (c) Balance voltage and (d) Temperatures.

quench. The operation currents of both the LTS and HTS coils started to decrease just after the quench event. The HTS current showed upturn around a few seconds. It is due to the balance between the dumping current and the induced current from the outer LTS coils. The similar behavior can be seen in the simulation results for the L1 coil quench. The current decay and coil voltages of the Gd123 coil continuously changed with time until around 6 s. However, the Gd123 current suddenly dropped around 6s and the vacuum pressure jumped up about two order magnitude. This suggests that the burn-out of the coil happened at this time. The current decay behaviors of HTS coil before 6 s is qualitatively similar to the simulation results of the L1 coil [24]. Therefore, it is suggested that the Gd123 coils were kept without the burn-out. This is a surprised phenomenon because many studies suggests that the hotspot in the local area in Gd123 coils gives rise to a serious damage and burn-out of the coil in the adiabatic condition. We may find a good solution to keep the Gd123 coil at least in a few seconds and a good quench protection of practical RE123 coils.

C. Bi2223 insert coil [20]

The Bi2223 insert was tested without a background field first. We successfully generated a 11.60 T with the operation current of 204.7 A without any problems [20]. The measured centering magnetic field is 11.48 T at 204.7 A, indicating about 0.12 T smaller than the expected value, originated from the sheading current effect. The maximum temperature of the Bi2223 coil was about 6 K at the stand-alone test. Then the combination tests were performed. At the virgin run, we energized the Bi2223 coil step-by-step under the background field of 14 T by the LTS coil as shown in Fig. 8. Unfortunately, we lost the data during the discharging because of the trouble of data acquisition system. Although large noise appeared during energizing, no anomalous voltage could be observed. Finally, a 24.64 T (calculated value) of centering field was achieved at 187.8 A successfully. For the discharge of the 25 T-CSM, both the currents of HTS and LTS magnets were decreased to zero simultaneously in about one-hour. Then we performed one-hour charging/discharging tests up to 24.64 T. This is a normal operation for users. The current vs balance voltage properties at the simultaneous sweep show no amorous voltage was observed as shown in Fig. 9. In this case, the maximum temperature of the HTS coil is also about 7 K. The measured magnetic field was 24.57 T at 187.8 A, indicating the field difference of 0.07 T as shown in Fig 10.

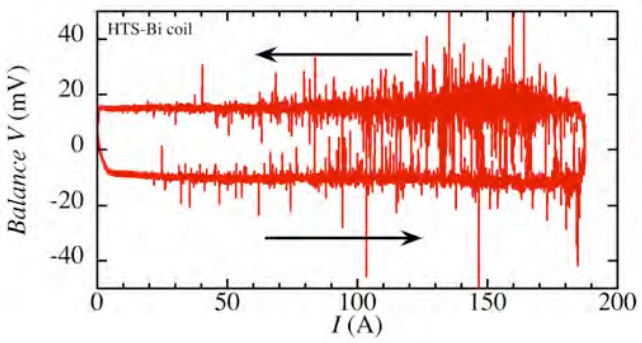

Fig. 9. Current vs balance voltage properties of the Bi2223 coil with the simultaneous sweep of the 25T-CSM.

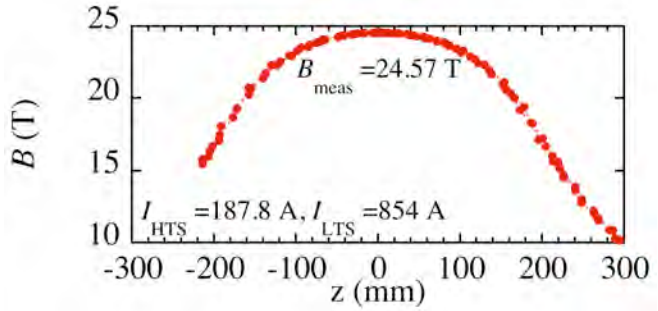

Fig. 10. Current vs balance voltage properties of the Bi2223 coil with the simultanous sweep of the 25T-CSM

Since the guaranteed magnetic field of the 25 T-CSM is 24.5 T, we carried out the performance test up to 24.64 T this time. But the hoop stress and I_c have still room to generate 25.0 T, because we have checked the hoop-stress up to that corresponding 25.0 T using the R&D two double pancake coils [17].

D. Magnetic field hysteresis

The central magnetic field hysteresis behaviors were observed in both the Gd123 and the Bi2223 inserts as shown in Fig. 11. The difference between the measured and calculated magnetic field around 24 T is about 0.41 T in the Gd123 insert coil. It is larger than 0.07 in the Bi2223 coils. In addition, the hysteresis behaviors of magnetic fields are different depending on the field-charging method. Therefore, it is difficult to know the magnetic field at the sample space. In order to monitor the present magnetic field, the Cu bifilar twisted wound coil is set in the bobbin of the Bi2223 insert. In this case, the present magnetic field can be measured by the magnet resistance of Cu. The good relationship between the resistance and measured magnetic field can be seen as shown in Fig. 12.

E. Experiments using the 25T-CSM

We measured the J_c properties of Sm123 films with $BaHfO_3$ nanorods for a trial use [25-27]. The example of *I-V* data at 4.2 K and 24.4 T for various field angles are shown in Fig. 13. The noise level is less than 0.1 μV, which is one order smaller than those in hybrid magnets. In addition, we can hold a long experimental time in high magnetic fields beyond 20 T.

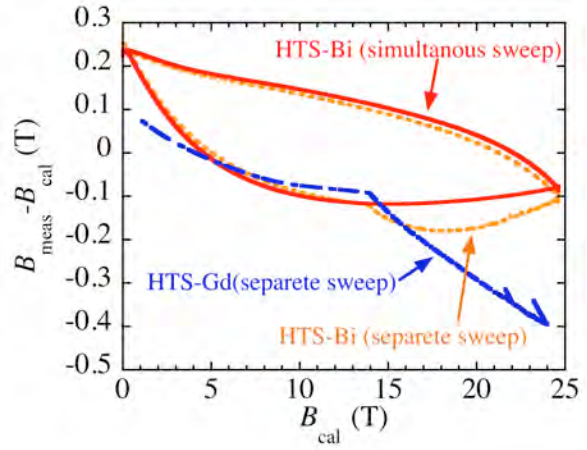

Fig. 11. Magnetic field histeresis of the 25T-CSM.

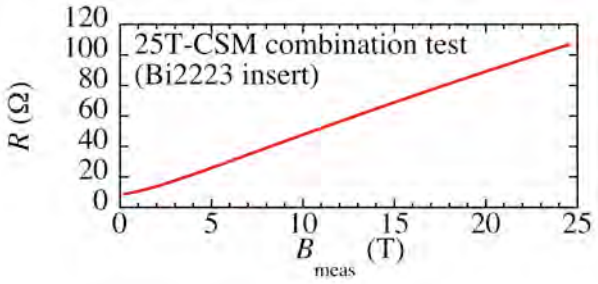

Fig. 12. Magnetic field monitor signal as a function of measured field.

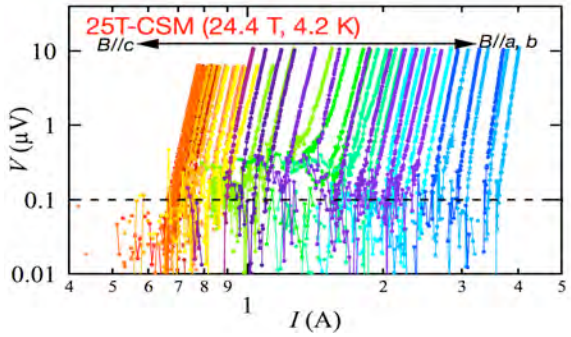

Fig. 13. *I-V* mearements for anguler depedence of J_c for a Sm123 film at 4.2 K and 24.4 T.

A ^{3}He, a ^{4}He and a gas flow cryostats and a furnace have been installed. A dilution refrigerator will be also installed to the 25 T-CSM in near future. Various experiments with a high stability and a long time are avairable using the 25T-CSM soon.

VI. Conclusion

We have been developed and installed the 25 T cryogen-free superconducting magnet (25T-CSM) at the High Field Laboratory for Superconducting Materials, IMR, Tohoku University. The 25T-CSM consists of the inner HTS, the middle Rutherford Nb_3Sn and the outer NbTi Rutherford cable magnets. We made the Gd123 and Bi2223 insert coils as the HTS insert for 25T-CSM. We achieved a 24.01 T by the Gd123 insert in a 14 T background field by the LTS coil but quenched just after the 24T generation. The quench behavior of the Gd123 coil suggests that we may have a time about 6 s after the thermal-runaway. The solution of quench protection may be found based on the obtained results. A 24.6 T was achieved by the Bi2223 insert combined with a 14 T of LTS outsert magnet, successfully. In this case difference between the calculated and measured magnetic fields was about 0.07 T at 24.64 T, although it is about 0.40 T in the case of the Gd123 insert. The magnetic field monitor using Cu is effective to know the present magnetic fields.

References

[1] S. Awaji *et al.*, "New 25 T Cryogen-Free Superconducting Magnet Project at Tohoku University," IEEE Trans. Appl. Supercond., **24** (2014) 4302005.
[2] H. W. Weijers *et al.*, "Progress in the Development of a Superconducting 32 T Magnet With REBCO High Field Coils," IEEE Trans. Appl. Supercond., **24** (2014) 4301805.
[3] S. Yoon *et al.*, "26T 35mm all-$GdBa_2Cu_3O_{7-x}$ multi-width no-insulation superconducting magnet," Supercond. Sci. Technol., 29 (2016) 04LT04 (6pp).

[4] C. Barth *et al.*, "Electro-mechanical properties of REBCO coated conductors from various industrial manufacturers at 77 K, self-field and 4.2 K, 19 T," Supercond. Sci. Technol., **28** (2015) 045011.
[5] https://nationalmaglab.org/
[6] T. Nakashima *et al.*, "Drastic Improvement in Mechanical Properties of DI-BSCCO Wire With Novel Lamination Material," IEEE Trans. Appl. Supercond., **25**, (2015) 6400705.
[7] Y. Miyoshi *et al.*, "Hoop stress test on new high strength alloy laminated Bi-2223 conductor,"Supercond. Sci. Technol., **28** (2015) 075013.
[8] S. Awaji et al., "Repairing and upgrading of the HTS insert in the 18T cryogen-free superconducting magnet," Adv. Cryo. Eng., **59** (2014) 732-739.
[9] S. Hanai, *et al.*, "Upgraded Cryogen-Free 20 T Superconducting Magnet," IEEE Trans. Appl. Supercond., **24**, (2014) 4301204.
[10] S. Awaji *et al.*, "Magnetic Field Quality Evaluation of a 20-T Cryogen-Free Superconducting Magnet With a Bi2223 Insert," IEEE Trans. Appl. Supercond., **26** (2016) 4701104 (4pp).
[11] G. Nshijima *et al.*, "Operation of 1020-MHz NMR Superconducting Magnet 1020MHz," IEEE Trans. Appl. Supercond., **26**, (2016) 4303304.
[12] H. Oguro," Mechanical and superconducting properties of Nb_3Sn wires with Nb-rod-processed CuNb reinforcement," Supercond. Sci. Technol. **26** (2013) 094002 (4pp).
[13] M. Sugimoto *et al.*, "Development of Nb-Rod-Method Cu–Nb Reinforced Nb_3Sn Rutherford Cables for React-and-Wind Processed Wide-Bore High Magnetic Field Coils," IEEE Trans. Appl. Supercond., **25** (2015) 6000605 (4pp).
[14] H. Oguro *et al.*, "Performance of a 14-T CuNb/Nb3Sn Rutherford coil with a 300mm wide cold bore," Supercond. Sci. Technol. **29** (2016) 084004 (5pp).
[15] K. Takahashi *et al.*, "Internal Strain Measurement for a Nb_3Sn Rutherford Cable Using Neutron Diffraction," IEEE Trans. Appl. Supercond., **25** (2015) 8400104 (4pp).
[16] H. Oguro *et al.*, "Transport Properties of CuNb Reinforced Nb_3Sn Rutherford Coils in High Fields," IEEE Trans. Appl. Supercond., **25** (2015) 8800104 (4pp).
[17] S. Awaji *et al.*, "10T generation by an epoxy impregnated GdBCO insert coil for the 25T-cryogen-free superconducting magnet," Suprerocnd. Sci. Technol., **29** (2016) 05510 (5pp).
[18] T. Takematsu *et al.*, "Degradation of the performance of a YBCO-coated conductor double pancake coil due to epoxy impregnation," Physica C **470** (2010) 674.
[19] H. Miyazaki *et al.*, "Degradation free impregnated YBCO pancake coils by decreasing radial stress in the windings and method for evaluating delamination strength of YBCOcoated conductors," IEEE Trans. Appl. Supercond., **24** (2014) 4600905.
[20] S. Hanai *et al.*, "Development of an 11T BSCCO Insert Coil for a 25T Cryogen-free Superconducting Magnet," presented to ASC2016, 4LPo1D-01.
[21] M. Takahashi *et al.*, "Design and test results of a cryogenic cooling system for a 25T cryogen-free superconducting magnet," ASC2016, 3LPo2B-04.
[22] S. Awaji *et al.*, "AC Losses of an HTS Insert in a 25-T Cryogen-Free Superconducting Magnet," IEEE Trans. Appl. Supercond., **25** (2015) 4601405 (5pp).
[23] http://www.shicryogenics.com//wp-content/uploads/2012/11/RDK-415D_Capacity_Map.pdf
[24] H. Miyazaki *et al.*, "Design of a REBCO Insert Coil for a Cryogen-Free 25-T Superconducting Magnet," IEEE Trans. Appl. Supercond., **25** (2015) 4603205 (4pp).
[25] Y. Yoshida *et al*, "Strongly enhanced vortex pinning in the SmBCO coated conductor with high density and fine inclined nanorods," presented to ASC 2016, 2MOr1C-05.
[26] S. Miura *et al.*, "J_c anisotropy at low measurement temperatures in $SmBa_2Cu_3O_y$ superconducting tapes with $BaHfO_3$ nano-rods controlled via low-temperature growth," presented to ASC 2016, 1MOr1B-02.
[27] Y. Tsuchiya *et al*., "Effect of Nano-rods on Vortex Pinning State in $BaHfO_3$ doped $SmBa_2Cu_3O_y$ Films Deposited by Low Temperature Growth Technique," presented to ASC 2016, 2MOr1C-02.